Planning of Fast EV Charging Stations on a Round Freeway

Xiaohong Dong, Yunfei Mu, *Member, IEEE*, Hongjie Jia, *Member, IEEE*, Jianzhong Wu, *Member, IEEE*, and Xiaodan Yu

***Abstract*—A novel planning method of fast electric vehicle (EV) charging stations on a round freeway was developed, considering the spatial and temporal transportation behaviors. A spatial and temporal model based on the origin-destination (OD) analysis was developed to obtain all the EV charging points (the location on the round freeway that an EV needs recharging due to the low battery capacity). Based on a shared nearest neighbor (SNN) clustering algorithm, a location determination model was developed to obtain the specific locations for EV charging stations with their service EV clusters. A capacity determination model based on the queuing theory was proposed to determine the capacity of each EV charging station. The round-island freeway in Hainan Island of China was employed as a test system to illustrate the planning method. Simulation results show that the developed planning method can not only accurately determine the most suitable locations for EV fast charging stations considering the travelling convenience of EV users, but also minimize the sum of waiting cost and charger cost.**

***Index Terms*—Charging station, electric vehicle (EV), planning, Shared Nearest Neighbor (SNN) clustering algorithm, spatial and temporal model.**

NOMENCLATURE

L7e	Quadricycle-four wheels, with a maximum unladen mass of 400 kg or 550 kg for goods carrying vehicles.
M1	Passenger vehicle, four wheels up to 8 seats in addition to the driver's seat.
N1	Goods-carrying vehicle, four wheels, with a maximum laden mass of 3500 kg.
N2	Goods-carrying vehicle, four wheels, with a maximum laden mass between 3500 kg and 12,000 kg.
Cap	The maximum capacity of EV battery.
SOC	The state-of-charge of EV battery.
SOC_i	The initial *SOC* at the freeway entrance.
SOC_c	The battery *SOC* when EVs need to recharge.
Ran_{mc}	The maximum travel range of an EV with its maximum battery capacity.
Ran_{ac}	The travel range with available battery capacity.
Ran_{rt}	The EV travel range in real time.
Ran_{sc}	The EV travel range with the SOC_c.
v	The average travel velocity of an EV.
Δt	The travelling time for the Ran_{rt}
$\boldsymbol{A}$	The EV OD matrix.
$\boldsymbol{P}$	The EV probability OD matrix.
$\boldsymbol{B}$	The EV number distribution vector at the entrances of the round freeway.
B_t	The total number of EV entering the freeway.
D_{od}	The distance between the origin and the destination locations.
D_{acs}	The distance between two adjacent EV charging stations.
$\boldsymbol{S}_c$	The set of charging points including the locations and times.
SR	The service radius of an EV charging station.
$\boldsymbol{C}(i)$	The corresponding cluster set of candidate location *i*.
$\boldsymbol{CS}$	The candidate location set.
L_s	The average queue length for an EV charging station.
W_q	The average waiting time of EV users at a specific charging station.

Manuscript received June 23, 2015; revised November 07, 2015 and February 23, 2016; accepted March 21, 2016. Date of publication April 21, 2016; date of current version September 16, 2016. This work was supported in part by UK-China NSFC/EPSRC EV project under Grants 51361130152 and EP/L001039/1, in part by the National Natural Science Foundation of China project under Grants 51307115 and 51377117, in part by the National High Technology R&D Program (863) of China under Grant 2015AA050403, and in part by the Tianjin Municipal Science and Technology Development Program of China under Grant 15JCQNJC43500. Paper no. TSTE-00534-2015. *(Corresponding author: Yunfei Mu.)*

X. Dong, Y. Mu, H. Jia, and X. Yu are with the Key Laboratory of Smart Grid of Ministry of Education, Tianjin University, Tianjin 300072, China (e-mail: dongxiaohong@tju.edu.cn; yunfeimu@tju.edu.cn; hjjia@tju.edu.cn; yuxd@tju.edu.cn).

J. Wu is with the School of Engineering, Cardiff University, Cardiff CF24 3AA, U.K. (e-mail: wuj5@cardiff.ac.uk).

Color versions of one or more of the figures in this paper are available online at http://ieeexplore.ieee.org.

Digital Object Identifier 10.1109/TSTE.2016.2547891

I. INTRODUCTION

WITH the growing concerns over the energy depletion and environmental issues around the world, more and more attention is being paid to replace the fuel based automobiles with electric vehicles (EVs) which have the characteristics of zero-emission and low noise. As a result, a number of countries have taken specific initiatives to de-carbonize their transport sectors by developing their EV industry. In China, a relatively conservative development plan with the goal of increasing EVs ownership number to five millions by 2020 has been brought forward [1]. The government issued an "Energy saving and new energy automobile industry development plan" in June 2012, which set specific arrangements for the popularization and application of EVs in the future [1]. However, whether the EVs charging infrastructure will be available and convenient or not is a key factor that affects the future development and popularization of the EVs. And in true chicken-or-the-egg fashion, the lack of EV charging infrastructure will deter the widespread use of EVs. Thus, the related guidance has been put forward to build a convenient EV charging infrastructure

network, especially the fast charging stations on the freeways, which can significantly increase the EV travel range [2].

The planning methods for oil/gas stations have gradually been moving towards a standardization and legalization direction in order to satisfy the refueling demand of the fuel based automobiles [3], [4]. However, new factors impact on the locations and capacities of EV charging stations, such as the battery type and capacity, charging power and travelling behaviors of EV users [5]. Compared with the existing oil/gas stations, it is inevitable to develop new planning methods to determine the optimum locations and capacities of EV charging stations considering the above factors, where both the charging convenience and infrastructure cost are considered. Related research on the planning methods of EV charging stations has already been carried out.

To provide proper guidance for the deployment of EV charging stations, forecasting of the EV charging demand is needed. References [6]–[8] focus on the forecast models of EV charging load, which take the travel uncertainties into consideration. A mathematical model of EV charging load based on the fluid dynamic traffic model and the M/M/s queuing theory was developed in [9] to capture the dynamics of EV charging demand in a freeway EV charging station. The driving patterns are well addressed for the charging convenience based on the traffic flow density. In [10] and [11], an integrated method was developed for EVs impact assessment on load curves and network congestion, combining power system models, agent based transport simulations and modeling of specific vehicle technologies. A Spatial–Temporal model (STM) was developed in [12], which is an analysis method to model EV mobility both spatially and temporally to evaluate the impact of a large scale deployment of EVs on urban distribution networks. In references [13]–[16], the EV charging load was allocated to each charging station in an EV charging network based on different mechanisms considering the transportation behaviors to provide quality charging services to the EV users. In [17], a two-step screening method considering the environmental factors and the service radius of EV charging stations was proposed to determine the optimal sites of EV charging stations, and then an optimal sizing model for EV charging stations was developed. In [18], an optimal siting and sizing method was developed, where the locations and the number of chargers in each charging station are determined at the same time considering the charging demand. In [19], a Mixed-Integer Non-Linear (MINLP) optimization approach was proposed for optimal placing and sizing of the fast charging stations at the urban roads to minimize the total cost of charging station development. In [20], the specific architecture in the interior of EV charging station with a single AC/DC conversion and a DC distribution to DC/DC charging units was discussed.

The existing research work has made good contributions to the planning of EV charging stations from different perspectives, such as charging demand modelling, grid impact analysis of EVs considering the transportation behaviors, and charging station planning. However, the following critical aspects have not yet been studied in details.

1) The uncertainties regarding the transportation behaviors of EV users introduce a spatial and temporal characteristic to the EV charging points, which is critical to determine the optimum locations of EV charging stations.
2) The planning of EV charging stations should capture the locations with the maximum EV charging demand, which can improve the convenience of EV users.
3) The EVs receive charging service at the charging stations following a stochastic process, which impacts the capacity (cost) of each charging station.

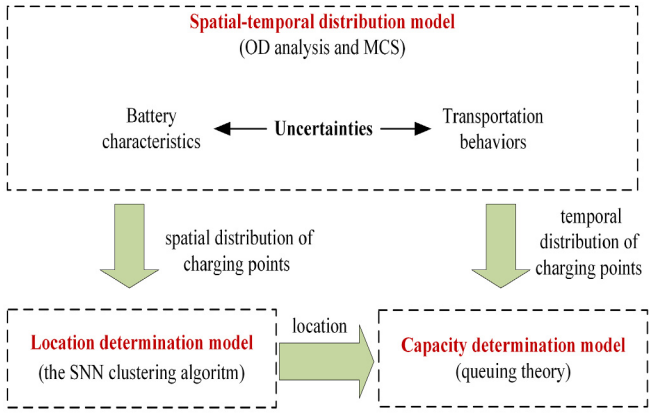

Fig. 1. Framework of the planning method.

To solve above problems, a novel planning method of fast EV charging stations on a freeway was proposed, which consists of a spatial-temporal model, a location determination model and a capacity determination model, to determine the locations and sizes of the EV charging stations and improve the convenience of EV users with a lower planning cost. The STM introduced in [12] was further developed in the proposed planning method to model the spatial and temporal transportation behaviors of vehicles on the freeway".

II. Framework of the Planning Method

The framework of the planning method is shown in Fig. 1, which is decomposed into three parts: a spatial-temporal model of EV charging points, a location determination model and a capacity determination model of EV charging stations.

1) **Spatial-temporal model:** The STM developed in [12] was further developed to consider the geographic information of the freeway. The MERGE EV database provides the characteristics of battery type, capacity and the maximum travel range of EVs [21]. The Origin-Destination (OD) analysis is used to model the transportation behaviors of EV users, i.e. to obtain the origin and the destination locations of each EV and the corresponding travel distance, *etc*. The information supplied by the battery characteristics and transportation behaviors is used by the Monte Carlo simulation (MCS) to obtain the spatial-temporal distribution of all the EVs charging points considering the above uncertainties.
2) **Location determination model:** The Shared Nearest Neighbor (SNN) Clustering algorithm is implemented to obtain the number and locations of EV charging stations

through the spatial distribution of the EV charging points (supplied by the spatial-temporal model).

3) **Capacity determination model:** The capacity of each EV charging station (represented by the amount of chargers) is optimized using the queuing theory through the temporal distribution of the EV charging points (supplied by the spatial-temporal model) with the corresponding location.

III. The Planning Method

A. Spatial-Temporal Model

1) Modelling the Uncertainties of EV Batteries: Based on a depth survey of the worldwide EV battery market, four types of EVs were identified in the EV database based on the type of vehicles: L7e, M1, N1 and N2 [21].

The battery capacity: According to the EV database, the probability density functions (*pdf*) of EV battery capacity (*Cap*) of different EV types (L7e, M1, N1 and N2) used in the MCS are shown in (1)-(2). The parameters of each *pdf* are defined by (1) for Gamma distribution and (2) for Normal distribution [21]. For each EV, the MCS is used to generate *Cap* based on the corresponding *pdf* and constraints. If the capacity generated is outside the maximum (Max) and minimum (Min) kWh constraints, the process is repeated until the constraints are satisfied.

$$f\left(Cap,\alpha,\beta\right)=\frac{1}{\beta^{\alpha}\Gamma\left(\alpha\right)}Cap^{\alpha-1}e^{-\frac{Cap}{\beta}} \tag{1}$$

$$g\left(Cap,\mu,\sigma\right)=\frac{1}{\sigma\sqrt{2\pi}}e^{-(Cap-\mu)^2/2\sigma^2} \tag{2}$$

where α and β are the shape parameter and scale parameter of the *pdf* of Gamma distribution, respectively; μ and σ are the mean and standard deviation of the *pdf* of Normal distribution.

The travel distance: The EV database provides the maximum travel range of an EV with its maximum battery capacity (Ran_{mc}) for different types of EVs. The mathematical relationship between Ran_{mc} and *Cap* is determined by polynomial fitting [12].

It is assumed that the *SOC* varies linearly with the real travel distance [22]–[24]. The travel range with available battery capacity (Ran_{ac}) of an EV is depicted in (3) and the EV travel range with the SOC_c (Ran_{sc}) of an EV is depicted in (4).

$$Ran_{ac}=\eta\times\left(SOC_i-SOC_c\right)\times Ran_{mc} \tag{3}$$

$$Ran_{sc}=\eta\times SOC_c\times Ran_{mc} \tag{4}$$

where η is an energy efficiency coefficient, which is introduced to consider the energy loss of an EV caused by the acceleration and deceleration processes. In this paper, it is assumed that the SOC_i varies in the range of [0.8, 0.9] (80%–90% SOC was used to maintain the life time of a battery from overcharge in [21]).

2) Modelling the Uncertainties of Transportation Behaviors: The uncertainties about the transportation behaviors can be simulated by the OD analysis [25]. The information needed by the OD analysis includes the geographic information of the planning area, the number of EVs, the travel starting time, and the OD matrix modelling EV mobility. The OD matrix is usually available in local transport departments and is obtained by transport survey or from intelligent transportation systems [24]–[26].

Geographic information: In this paper, the round freeways are used as the planning area. The entrances & exits on the round freeway are used as the origin and the destination for the OD analysis. It is assumed that the EV users select the shortest path for their travels with an average velocity (v), and the Floyd algorithm is used to determine the shortest path between the origin and the destination locations [27]. The travelling time (Δt) for the range in real time (Ran_{rt}) is depicted in (5).

$$\Delta t=\frac{Ran_{rt}}{v} \tag{5}$$

OD matrix: The daily travel on the round freeway usually follows a regular pattern. Each EV is assigned with an origin and a destination pair. In the MCS process, an OD matrix is used to model the EV mobility from entering the freeway to exiting the freeway for the whole trip [25]–[27].

The OD matrix $\boldsymbol{A}_{m\times m}$ is introduced in the OD analysis, where m is the total number of the entrances & exits on the round freeway. The element a_{ij} $(1\le i\le m, 1\le j\le m)$ in the $\boldsymbol{A}_{m\times m}$ represents the number of EVs travelling from the entrance (origin) i to the exit (destination) j. The $\boldsymbol{A}_{m\times m}$ is then converted to a probability OD matrix $\mathbf{P}_{m\times m}$ through (6).

$$p_{ij}=a_{ij}/B_i(1\le i\le m, 1\le j\le m) \tag{6}$$

$$B_i=\sum_{j=1}^{m}a_{ij}(1\le i\le m, 1\le j\le m) \tag{7}$$

$$B_t=\sum_{i=1}^{m}B_i(1\le i\le m) \tag{8}$$

where p_{ij} in $\boldsymbol{P}_{m\times m}$ is the probability of EV travelling from the origin i to the destination j; B_i represents the number of EV entering the freeway from the entrance i; B_t is the total number of EVs entering the freeway.

Due to the fact that the OD analysis method used in this section for transportation simulation is independent from the road topologies [12], the spatial and temporal model can be used for any road topology, although the freeway is focused in this paper.

The travel starting time: The travel starting time (t_s) is determined based on the travel starting time distribution, which is obtained from the statistical survey [28].

3) Flow Chart of the Spatial-Temporal Model: The spatial and temporal distribution of EV charging points is then obtained through the MCS process, which is shown in Fig. 2. Part I deals with the uncertainties of battery characteristics, part II deals with the uncertainties from transportation behaviors of EV users, and part III includes the steps tracking the EVs mobility to obtain the charging times and the locations of different EV charging points. Actually, whether an EV needs to recharge or not during its travel route depends on the relationship between Ran_{ac} and D_{od}. If Ran_{ac} is larger than D_{od}, the EV can finish its travel without any recharging process. While if Ran_{ac} is smaller than D_{od}, the EV needs at least one recharging process in order to reach its destination.

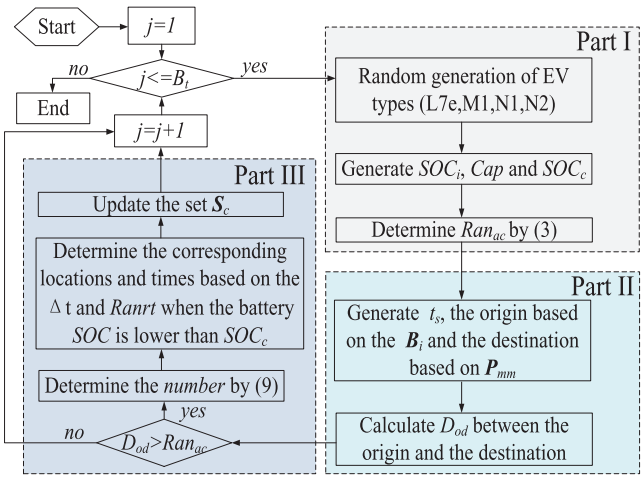

Fig. 2. The flowchart of the spatial-temporal model.

Part I: This part is used to generate the battery parameters (EV type, SOC_i, SOC_c, *Cap*) for each EV entering the freeway by using the MCS process, and Ran_{ac} is then determined by (3).

Part II: This part is used to generate the initial location, travel destination and t_s for each EV by using the MCS process based on the probability OD matrix $\boldsymbol{P}_{m\times m}$ depicted in (6). Then D_{od} is obtained by the real distance between the origin and the destination according to the geographic information.

Part III: This part is used to determine all the charging locations and times for an EV along its travelling route. The number of charging locations (*num*) is firstly determined by (9).

$$num = fix(D_{od}/Ran_{ac}) \tag{9}$$

where the function '*fix*' means rounds the value of (D_{od}/Ran_{ac}) to the nearest integer towards zero.

The EV needs to recharge when the battery SOC is lower than SOC_c. The corresponding charging locations and times are then determined based on Δt and Ran_{rt}. More details can be found in [12]. It provides the detailed process of the spatial temporal model which forms the basis for the determination of the locations and times of the charging points.

The spatial distribution of charging points $\boldsymbol{S}_c$ is then transmitted to the location determination model and capacity determination model of EV fast charging station.

B. Location Determination Model

A location determination model based on the SNN algorithm was developed, which determines the number and locations of EV fast charging stations through the spatial distribution of EV charging points (supplied by the spatial-temporal model) considering the service radius (*SR*) of each EV charging station.

1) SR Determination: The locations of EV fast charging stations should satisfy the charging convenience of EV users. As a result, a *SR* is introduced to guarantee each EV can drive to an adjacent charging station with SOC_c. Based on the Ran_{sc} distribution supplied by the spatial-temporal model, the *SR* is determined.

1) Determine the distribution of Ran_{sc} by using the normal fitting as depicted in (10) according to the central limit theorem in probability theory [29].

$$\theta\left(Ran_{sc}, \mu_1, \sigma_1\right) = \frac{1}{\sigma\sqrt{2\pi}} e^{-(Ran_{sc}-\mu_1)^2/2{\sigma_1}^2} \tag{10}$$

where μ_1 and σ_1 are the mean and standard deviation of the normal probability density function, respectively.

2) Determine the *SR* based on the normal distribution of Ran_{sc} with (1-a%) confidence level, which is depicted in (11).

$$SR = \mu_1 - b \times \sigma_1 \tag{11}$$

where μ_1 and σ_1 are the mean value and standard deviation of the Ran_{sc} distribution, respectively; b is the coefficient determined by lookup of the standard normal distribution function table corresponding to (1-a%). It means that (1-a%) of EVs can travel to a fast charging station within *SR* with SOC_c.

In order to avoid redundant planning, the minimum distance between two adjacent EV charging stations (D_{acs}) follows the constraint depicted in (12).

$$D_{acs} \geq SR \tag{12}$$

2) The SNN Clustering Algorithm: The locations of EV fast charging stations are determined according to the EV charging points supplied by the spatial-temporal model, based on the SNN algorithm proposed in [30] and [31], which is shown in Fig. 3.

Step I: Calculate the distance (d_{ij}) between any two charging points. A distance matrix $\boldsymbol{D}$ with *n*-dimension is formed by *n* charging points, where the d_{ij} is the element in $\boldsymbol{D}$.

Step II: Determine the similarity matrix $\boldsymbol{S}$ (with *n*-dimension) of the charging points. The matrix element s_{ij} in $\boldsymbol{S}$ is defined in (13).

$$\begin{aligned} s_{ij} &= \text{size}\left(\boldsymbol{NN}(i) \cap \boldsymbol{NN}(j)\right) \quad 1 \leq i, j \leq n, i \neq j \\ s_{ii} &= 0 \end{aligned} \tag{13}$$

where $\boldsymbol{NN}(i)$ is a set of charging points within the radius of *SR* of the charging point *i*; $\boldsymbol{NN}(j)$ is a set of charging points within the radius of *SR* of the charging point *j*; The "size" means the shared number of charging points in the intersection set of $\boldsymbol{NN}(i)$ and $\boldsymbol{NN}(j)$.

Step III: Calculate the EV charging demand of each charging point, which is determined by the total shared number of charging points. The similarity vector $\boldsymbol{L}_{1\times n}$ is defined in (14) as the EV charging demand for each EV charging point.

$$l_{1,j} = \sum_{i=1}^{n} s_{ij} (1 \leq j \leq n) \tag{14}$$

where *n* is the number of charging points; $l_{1,j}$ is the EV charging demand at the charging point *j*.

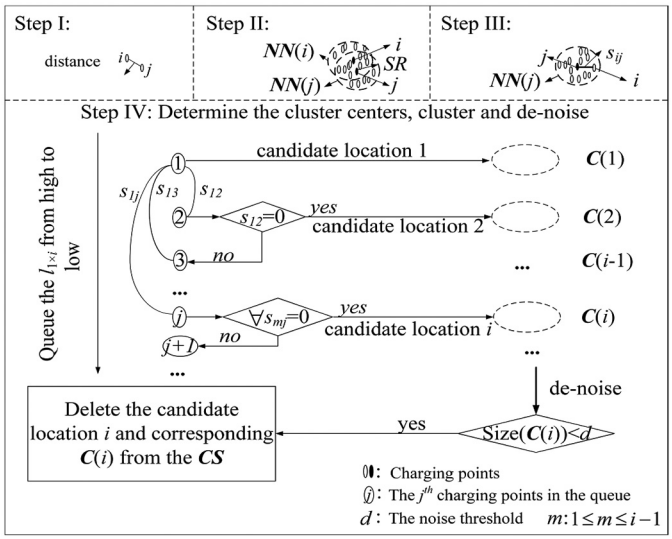

Fig. 3. The SNN clustering algorithm.

Step IV: Determine the cluster centers, cluster and de-noise.

1) Queue the elements in $\boldsymbol{L}_{1\times n}$ based on the EV charging demand ($l_{1,j}$) from high to low. The charging point with the largest charging demand is taken as the first cluster center, namely the 1-th candidate location of EV fast charging station. At same time, a cluster set $\boldsymbol{C}(1)$ is determined, which includes the charging points within the service radius of the 1-th candidate location. Then, the candidate location set $\boldsymbol{CS}$ is updated, which includes the 1-th candidate location with its cluster set $\boldsymbol{C}(1)$.
2) The next charging point *j* is judged whether the similarities between the charging point *j* and the determined candidate locations are zero or not. If the similarities all equal to zero, the charging point *j* is chosen as the *i*-th candidate location, and its cluster set $\boldsymbol{C}(i)$ is also determined. Meanwhile the $\boldsymbol{CS}$ is updated. This process is repeated until all the EV charging points are judged one by one.
3) If the number of elements in the cluster set $\boldsymbol{C}(i)$ of the candidate location *i* is less than a predefined noise threshold d, the candidate location *i* and the corresponding $\boldsymbol{C}(i)$ is deleted from the $\boldsymbol{CS}$. The remaining candidate locations in $\boldsymbol{CS}$ are the final EV fast charging station locations.

C. Capacity Determination Model

It is assumed the amount of chargers (i.e. the capacity of a charging station) of each EV charging station should satisfy the peak number of EVs to be charged, arriving at the corresponding fast charging station per hour. As a result, a capacity determination model based on the queuing theory was developed to determine the amount of chargers in each charging station.

1) EV Queuing Model: It is assumed that the charging service of each EV at a specific charging station is independent to each other and the capacity optimization of charging station belongs to a standard $\mathrm{M/M/C/\infty/\infty}$ queuing problem [32]–[34]. Based on the queuing theory, the average queue length (L_s) is determined by (15) $\sim$ (17). The average waiting time (W_q) is determined by (18).

$$L_s = L_q + \frac{\lambda}{\mu_2} = \frac{(c\rho)^c \rho}{c!(1-\rho)^2} P_0 + \frac{\lambda}{\mu_2} \tag{15}$$

$$P_0 = \left[\sum_{k=0}^{c-1} \frac{1}{k!} \left(\frac{\lambda}{\mu_2}\right)^k + \frac{1}{c!} \frac{1}{1-\rho} \left(\frac{\lambda}{\mu_2}\right)^c \right]^{-1} \tag{16}$$

$$\rho = \lambda/(c \cdot \mu_2) \tag{17}$$

$$W_q = \frac{L_q}{\lambda} \tag{18}$$

where c is the number of chargers in the charging station; λ is the parameter of Poisson distribution representing the arrival EV number at peak hour; μ_2 is the parameter of Exponential distribution representing the average service rate of a charger per hour.

The idle proportion of chargers in a charging station is described in (19).

$$I_0 = (1 - \frac{\lambda}{c\mu_2}) \times 100\% \tag{19}$$

2) Capacity Optimization: It is assumed that all the chargers have the same power rating. Any charger can satisfy the charging requirement of a single EV battery at a specific time. If the number of chargers in a charging station is the maximum EV number per hour, the cost for the chargers is increased, while the waiting cost of EV users is reduced, and vice versa. As a result, the charger number should be optimized considering both the charger cost and waiting cost.

The cost of an EV charging station usually consists of station equipment cost (i.e. chargers in this paper), land cost and other costs (e.g. labor costs). The charger cost is assumed to vary linearly with the station capacity which itself is a function of the amount of chargers installed in the station [19]. A capacity optimization model depicted in (20) was developed to coordinate the charger cost and the waiting cost for an EV charging station, which minimizes the sum of the charger cost and the waiting cost of the EV users. The upper limit of W_q is shown in (21). The cost of one charger considering its life-cycle was converted to per hour (C_s) and depicted in (22). The cost associated with other basic equipment, the land cost and other costs were considered as the fixed cost, which are not included in (20). c is the decision variable of this optimization model representing the charger number.

$$\min z = C_s c + C_w L_s \tag{20}$$

$$s.t.\, W_q < t_w \tag{21}$$

where z is the total cost; C_w is the time cost per hour for each EV user in a charging station through the survey [35]; t_w is a constant of waiting time.

$$C_s = V_0 \frac{i_r(1+i_r)^p}{(1+i_r)^p - 1}/8760 \tag{22}$$

where V_0 is the cost for each charger in life-cycle; i_r is the interest rate; *p* is the life-cycle of a charger.

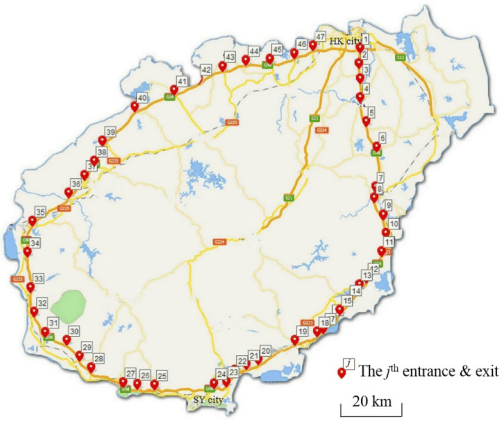

Fig. 4. The round-island freeway of Hainan with entrances & exits.

IV. Test Case

Hainan Island locates at the southern coast of China in the South China Sea, which is famous for its fabulous natural scenery and considered as a 'South Sea Pearl' in China. The construction aim of Hainan Island is to build an international tourist island, which has risen to a Chinese national strategy [36]. For this reason, the development of EVs has become an important issue in Hainan's low carbon economy in recent years. The round-island freeway is one of the main frameworks of freeway in Hainan Province, which significantly affects the comprehensive transportation ability and has a profound influence on the eco-economic development of Hainan Island. In order to accommodate the increasing EV number in Hainan Island, it is necessary to construct a convenient EV fast charging station network for the round-island freeway, which has become a key development objective at the government level in Hainan Island.

A. Test System and Simulation Parameters

The round-island freeway of Hainan Island shown in Fig. 4 is used as a test system, where the 47 red locations are the entrances & exits of the freeway. The following information is required to fill the simulation parameters for planning purpose.

1) Geographic Information: The distance between each entrance & exit and the reference entrance & exit (numbered 1 in the case study) with the coordinate values are given in Table I. Besides, twelve service areas owning oil stations on the round-island freeway are given in the shadow area of Table V.

2) EV Number at 2020: Based on the data from [28], there will be daily average 34594 vehicles travelling on the round island freeway at the year of 2020. It is assumed that 50% of vehicles will be replaced by EVs. As a result, it is estimated that there will be 17297 EVs travelling on the round-island freeway by 2020 [28], where it is assumed that L7e type accounts for 10%, M1 accounts for 84%, N1 accounts for 3%, and N2 accounts for 3%, according to the statistical data from [12].

3) Parameters for Monte Carlo Simulation and Optimization: The simulation parameters are listed in Table II. The probability density functions (*pdf*) of EV *Cap* of different EV types used in the MCS and constraints are shown in Table III, which are obtained based on a survey of the global EV market [12]. The mathematical relationship between Ran_{mc} and *Cap* is shown in Fig. 5, where the squares show the Ran_{mc} of each type of M1 EV versus its *Cap*, and the stars show the result of polynomial fitting. The travel starting time distribution along a day is shown in Fig. 6, which was extracted from [28]. The probability OD matrix $\boldsymbol{P}_{m\times m}$ used for transport simulation of the round-island freeway is shown

TABLE I
The Entrance & Exit of the Test System

No.	Distance (km)	Coordinate (*x*,*y*)	No.	Distance (km)	Coordinate (*x*,*y*)
1	0	(213, 184)	25	269	(137, 26)
2	9	(214, 177)	26	279	(119, 26)
3	18	(214, 169)	27	287	(111, 27)
4	28	(214, 160)	28	302	(105, 27)
5	41	(217, 149)	29	317	(93, 33)
6	56	(222, 138)	30	328	(83, 41)
7	78	(215, 112)	31	339	(67, 52)
8	84	(215, 109)	32	351	(63, 61)
9	94	(225, 106)	33	365	(62, 72)
10	105	(226, 98)	34	384	(60, 89)
11	115	(224, 89)	35	402	(63, 103)
12	132	(217, 76)	36	427	(79, 116)
13	137	(214, 73)	37	439	(87, 124)
14	148	(208, 66)	38	449	(91, 131)
15	155	(205, 61)	39	460	(95, 141)
16	162	(200, 56)	40	492	(110, 156)
17	169	(198, 53)	41	508	(129, 164)
18	186	(194, 51)	42	523	(140, 169)
19	195	(184, 47)	43	538	(151, 175)
20	208	(168, 38)	44	551	(161, 178)
21	215	(161, 36)	45	563	(173, 179)
22	221	(156, 33)	46	577	(180, 180)
23	229	(146, 27)	47	587	(184, 181)
24	237	(213, 184)	total	612	(193, 184)

TABLE II
Parameters for Simulation

Parameter	Value	Unit
SOC_i	R(0.8-0.9)	-
SOC_c	R(0.15-0.3)	-
v	90	km/h
	1	-
b	1.65	-
a	5%	-
V_0	24	10^4 RMB
B_t	17297	-
i_r	0.10	-
p	30	year
μ_2	6	-
d	90	-
C_w	17	RMB/h
t_w	20	min

$R(a, b)$ represents a random value in interval $[a, b]$.

TABLE III
The *pdf* of EV Battery Capacity in MCS

EV group	L7e	M1	N1	N2
Distribution	Gamma	Gamma	Normal	Normal
Parameter	=10.8 =0.8	=4.5 =6.3	=23.0 μ=9.5	=85.3 μ=28.1
Max(kW/h)	15.0	72.0	40.0	120.0
Min(kW/h)	5.0	10.0	9.6	51.2

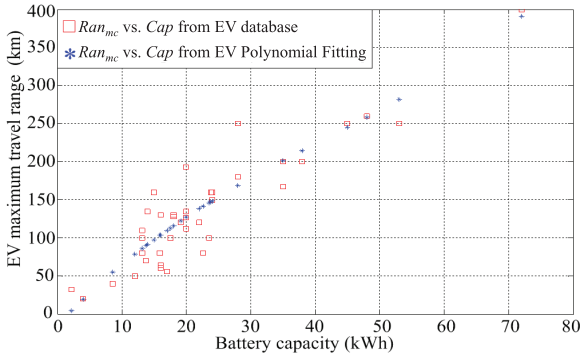

Fig. 5. The relationship between Cap and Ran_{mc}.

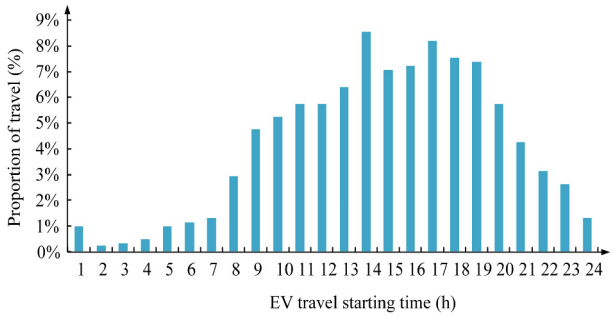

Fig. 6. EV travel starting time distribution along a day [28].

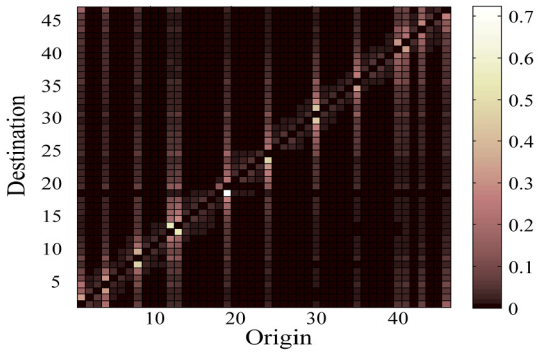

Fig. 7. The probability OD matrix of the round-island freeway [28].

in Fig. 7 extracted from [28], where the x-axis is the entrance where EVs enter the round-island freeway; y-axis is the exit where EVs leave the round-island freeway; the color bar at the right hand side represents the corresponding probability value. The distribution of Ran_{sc} by using the normal fitting is shown in the Fig. 8 and the service radius (*SR*) is determined.

In order to verify the effectiveness of the proposed planning method in this paper, two scenarios are considered in this section and the corresponding planning results are compared.

1) ***Scenario I***: determine the planning scheme of EV fast charging stations on the round-island freeway using the planning method developed in Section III.
2) ***Scenario II***: all the service areas (with the oil station) are selected as the charging stations firstly; and the locations and capacities of the remaining charging stations are determined using the method developed in Section III.

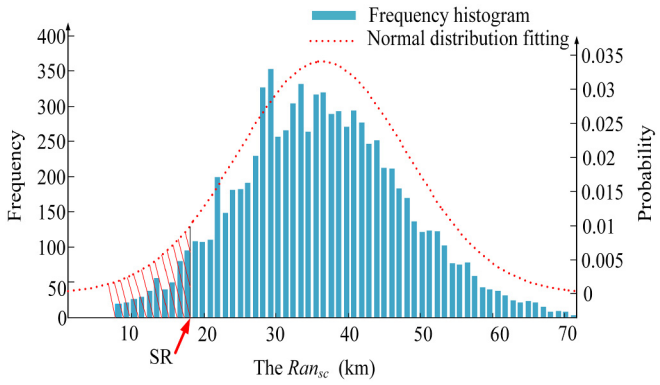

Fig. 8. The Ran_{sc} distribution.

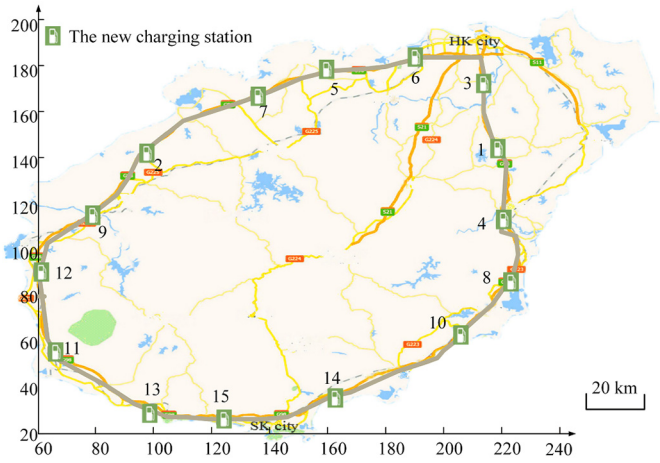

Fig. 9. The location of EV fast charging station of Scenario I.

In this part, selecting oil stations as the locations of EV charging stations firstly in Scenario II can not only verify the effectiveness of the planning method proposed in this paper by results comparison, but also reveal the fact that the locations of the existing oil/gas stations may not coincide with that of the charging stations due to the constraints of EV battery capacities.

B. Planning Results and Comparison

The planning scheme of charging stations under Scenario I is shown in Fig. 9, where the green squares are the planned charging stations. The planning scheme of charging station under Scenario II is shown in Fig. 10, where the red squares represent the planned charging stations in the existing service areas, and the green squares represent the new locations of charging stations. The planning scheme (the location, capacity and peak EV number) of each charging station are listed in Table IV (under Scenario I) and Table V (under Scenario II), respectively. The twelve shadow charging stations in Table V are constructed in the existing service areas.

The temporal distribution of the arrival EV number (charging demand) along a day at each charging station is shown in Figs. 11 and 12. It is obvious that the charging stations under

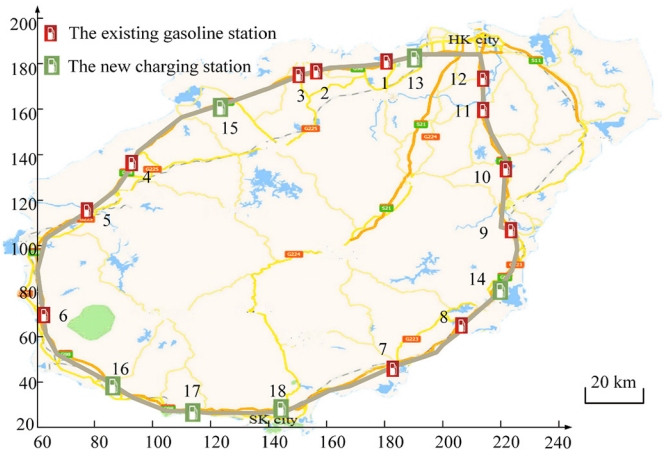

Fig. 10. The location of EV fast charging station of Scenario II.

TABLE IV
THE PLANNING SCHEME OF CHARGING STATION UNDER SCENARIO I

Charging station No.	Charger number	Coordination (*x, y*)	Distance (*km*)	Peak EV number per hour
1	31	(219.0, 144.6)	47.0	143
2	25	(97.1, 143.1)	436.5	113
3	24	(214.0, 173.7)	12.7	108
4	25	(220.4, 112.0)	81.3	111
5	24	(159.7, 177.6)	536.0	105
6	22	(190.1, 183.1)	583.8	94
7	22	(135.3, 166.9)	501.2	98
8	23	(222.9, 87.1)	117.5	101
9	19	(78.3, 115.5)	401.2	84
10	17	(206.2, 62.9)	152.3	73
11	18	(65.3, 55.8)	332.7	78
12	18	(60.3, 90.6)	367.2	79
13	19	(98.6, 30.2)	295.0	81
14	15	(162.2, 36.3)	213.8	64
15	14	(123.6, 26.0)	260.9	60

The distance in Tables IV and V means the distance between each charging station and the reference entrance & exit (numbered 1 in the case study).

TABLE V
THE PLANNING SCHEME OF CHARGING STATION UNDER SCENARIO II

Charging station No.	Charger number	Coordinate (*x, y*)	Distance (*km*)	Peak EV number per hour
1	18	(180.3, 180.1)	564.0	78
2	14	(156.3, 176.6)	531.0	60
3	17	(150.3, 174.6)	522.0	71
4	24	(93.0, 136.0)	444.0	105
5	19	(78.1, 115.3)	401.	84
6	19	(62.3, 68.3)	347.0	82
7	13	(181.5, 45.6)	197.0	55
8	15	(207.1, 64.6)	150.0	64
9	23	(223.5, 106.6)	91.0	103
10	27	(221.8, 133.2)	61.0	120
11	21	(214.0, 160.0)	28.0	91
12	19	(214.0, 174.3)	12.0	84
13	21	(190.1, 183.0)	583.8	93
14	23	(219.8, 81.2)	125.1	103
15	22	(123.3, 161.6)	482.4	97
16	17	(86.4, 38.3)	311.9	72
17	17	(113.8, 26.7)	275.5	74
18	17	(143.1, 26.7)	231.6	72

Scenario I can capture more charging demands than that of Scenario II. The related indexes and the differences between Scenario I and Scenario II are listed in Table VI. Compared with Scenario II, the planning scheme under Scenario I has the following two advantages.

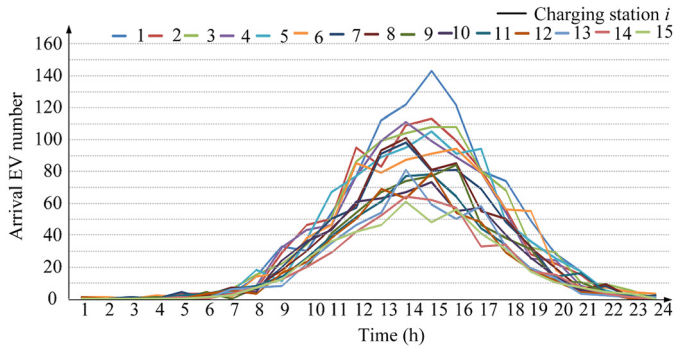

Fig. 11. The arrival EV number in each charging station under Scenario I.

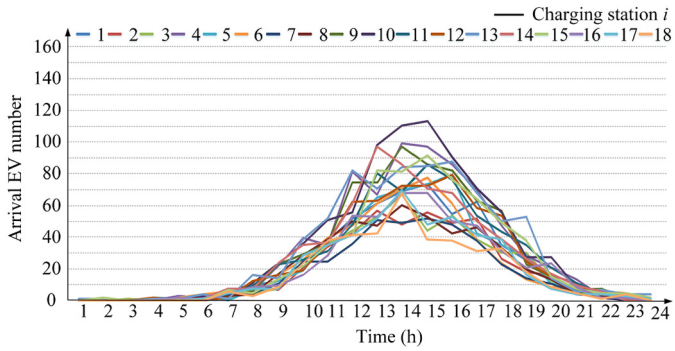

Fig. 12. The arrival EV number in each charging station under Scenario II.

TABLE VI
RELATED INDEXES ABOUT SCENARIO I AND SCENARIO II

	Scenario I	Scenario II	Difference
The charging station number	15	18	3
The charger number	316	346	30
Error*	2.46%	5.56%	3.1%
Total cost (million RMB/year)	43.36	47.16	3.80
Charger cost (million RMB/year)	8.03	8.79	0.76
Waiting cost (million RMB/year)	35.33	38.37	3.04

*The error is the percentage of EV charging points that are not covered by the planning scheme.

1) The planning scheme under Scenario I can cover more EVs' charging demand, which is depicted by the error index in Table VI.
2) The planning scheme under Scenario I not only can satisfy the EV charging points using less chargers, but also can minimize the infrastructure and waiting cost.

The idle proportions (I_0) for all the EV chargers under Scenarios I and II are depicted in Fig. 13. The idle proportions have a typical temporal distribution along a day, which have a close relationship with the distribution of EV travel starting time shown in Fig. 6. Besides, the planning scheme under Scenario I is able to improve the utilization of chargers at each charging station, especially during the period from 13 to 18 o'clock in the rush hours of the freeway. Figs. 14–15 show the idle proportion of chargers at the peak load time in each charging station, which further verifies the effectiveness of the proposed planning method in this paper.

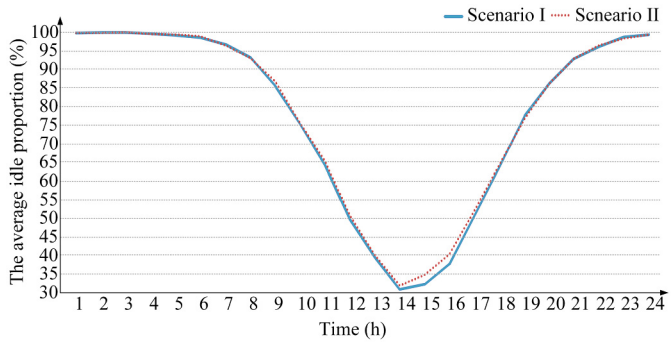

Fig. 13. The average idle proportion.

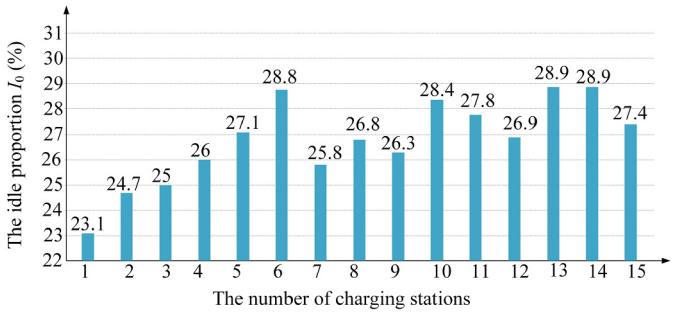

Fig. 14. The idle proportion at peak load time of Scenario I.

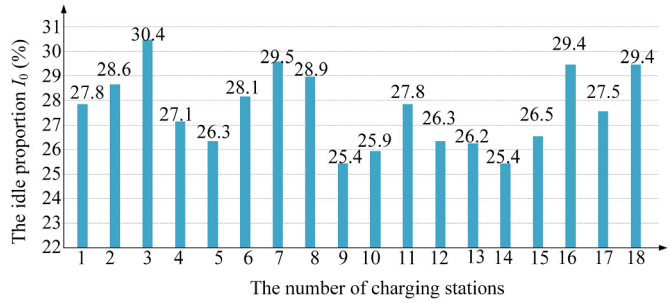

Fig. 15. The idle proportion at peak load time of Scenario II.

V. Conclusion and Further Work

A novel planning method of fast EV charging stations on a round freeway considering the spatial and temporal transportation behaviors is proposed.

The planning method is decomposed into three parts: a spatial-temporal model of EV charging points, a location determination model and a capacity determination model. The spatial-temporal model provides the EV charging points along the freeway considering the uncertainties of battery characteristics and transportation behaviors. The location determination model determines the optimum locations of EV fast charging stations by considering the spatial distribution of EV charging points, which is able to accurately capture the EV charging points and increase charging convenience of EV users. The capacity determination model determines the charger number in each charging station, which is able to minimize the sum of waiting cost and charger cost.

The round-island freeway of Hainan Island was used as a test system to illustrate the effectiveness of the proposed planning method. The following conclusions are given.

1) The uncertainties such as the battery characteristics and transportation behaviors of EV users are considered in the proposed planning method, which can accurately depict the EV charging points from a spatial and temporal perspective.
2) The developed planning method is able to capture the specific locations of EV charging demand in the planning area. Actually, the locations of the existing oil/gas stations may not coincide with that of the charging stations due to the constraints from battery capacities.
3) The developed planning method not only can accurately determine most suitable locations of EV charging stations considering the travelling convenience of EV users, but also can minimize the total cost.

However, the EV fast charging stations are not only public traffic infrastructure, but also power infrastructure. This paper mainly focuses on introducing the transportation characteristics to the planning method. Due to the long distance between any two EV charging stations on the round-island freeway of Hainan, each charging station is supplied by a separate distribution network around the freeway with sufficient capacity. As a result, the distribution network constraints were not considered in this paper. However, if grid reinforcements are needed to supply the increased charging capacity, the total infrastructure cost will change. Ref. [12] provides a method for grid impact analysis of EVs. An integrated planning model with multi-objectives and constraints should be developed if both charging infrastructure planning and network reinforcements are considered simultaneously. The future research will focus on building an integrated planning model also considering the constraints from electric networks.

References

[1] The State Council. (2012, Jun.). *Energy Saving and New Energy Automobile Industry Development Plan* [Online]. Available: http://www.nea.gov.cn/2012-07/10/c_131705726.htm
[2] The State Council. (2012, Jul.). *Guidance on Accelerating the Popularization and Application of New Energy Vehicles* [Online]. Available: http://www.gov.cn/zhengce/content/2014-07/21/content_8936.htm
[3] Ministry of Construction of the People's Republic of China. (Sep. 1995). *Code for Transport Planning on Urban Road*, GB 50220-95 [Online]. Available: http://www.spsp.gov.cn/page/CN/1995/GB%2050220-1995.shtml
[4] China Petroleum & Chemical Corporation. (Jun. 2012). *Code for Design and Construction of Filling Station*, GB 50156-5952002 [Online]. Available: http://www.spsp.gov.cn/page/CN/2012/GB%2050156-2012.shtml
[5] F. Xu, G. Q. Yu, L. F. Gu, and H. Zhang, "Tentative analysis of layout of electrical vehicle charging stations," *East China Electr. Power*, vol. 37, no. 10, pp. 1677–1682, Oct. 2009.
[6] S. Bae and A. Kwasinski, "Spatial and temporal model of electric vehicle charging demand," *IEEE Trans. Smart Grid*, vol. 3, no. 1, pp. 394–403, Mar. 2012.
[7] S. Shahidinejad, S. Filizadeh, and E. L. Bibeau, "Profile of charging load on the grid due to plug-in vehicles," *IEEE Trans. Smart Grid*, vol. 3, no. 1, pp. 135–141, Mar. 2012.
[8] A. Lojowska, D. Kurowicka, G. Papaehthymiou, and L. Sluis, "Stochastic modeling of power demand due to EVs using copula," *IEEE Trans. Power Syst.*, vol. 27, no. 4, pp. 1960–1968, Nov. 2012.
[9] W. Guibin, X. Zhao, W. Fushuan, and P. W. Kit, "Traffic-constrained multiobjective planning of electric-vehicle charging stations," *IEEE Trans. Power Del.*, vol. 28, no. 4, pp. 2363–2372, Oct. 2013.
[10] M. D. Galus *et al.*, "Integrating power system, transportation systems and vehicle technology for electric mobility impact assessment and efficient control," *IEEE Trans. Smart Grid*, vol. 3, no. 2, pp. 934–949, Jun. 2012.

[11] M. Galus and G. Andersson, "Demand management of grid connected plug-in hybrid electric vehicles (PHEV)," in *Proc. IEEE Energy 2030 Conf.*, Atlanta, GA, USA, Nov. 2008, pp. 1–8.
[12] Y. F. Mu, J. Z. Wu, N. Jenkins, H. J. Jia, and C. S. Wang, "A spatial temporal model for grid impact analysis of plug-in electric vehicles," *Appl. Energy*, vol. 114, pp. 456–465, Feb. 2014.
[13] G. Michailidis, M. Devetsikiotis, and F. Granelli, "Electric power allocation in a network of fast charging stations," *IEEE J. Sel. Areas Commun.*, vol. 31, no. 7, pp. 1235–1246, Jul. 2013.
[14] G. Michailidis, "Power allocation to a network of charging stations based on network tomography monitoring," in *Proc. 18th Int. Conf. Digital Signal Process. (DSP)*, Santorini, Greece, Jul. 2013.
[15] Y. C. Hung and G. Michailidis, "Optimal routing for electric vehicle service systems," *Eur. J. Oper. Res.*, vol. 247, pp. 515–524, 2015.
[16] I. Bayram, G. Michailidis, and M. Devetsikiotis, "Unsplittable load balancing in a network of charging stations under QoS guarantees," *IEEE Trans. Smart Grid*, vol. 6, no. 3, pp. 1292–1302, May 2015.
[17] Z. Liu, F. Wen, and G. Ledwich, "Optimal planning of electric-vehicle charging stations in distribution systems," *IEEE Trans. Power Del.*, vol. 28, no. 1, pp. 102–110, Jan. 2013.
[18] L. Jia, Z. Hu, Y. Song, and Z. Luo, "Optimal siting and sizing of electric vehicle charging stations," in *Proc. IEEE Int. Electr. Veh. Conf.*, Greenville, SC, USA, Mar. 2012, pp. 1–6.
[19] S. B. Payam, R. G. Abbas, and K. K. Hosein, "Optimal fast charging station placing and sizing," *Appl. Energy*, vol. 125, no. 214, pp. 289–299, 2014.
[20] S. Bai, D. Yu, and S. Lukic, "Optimum design of an EV/PHEV charging station with dc bus and storage system," in *Proc. Energy Convers. Congr. Expo. (ECCE)*, Sep. 2010, pp. 1178–1184.
[21] EU Merge Project. (2010). *Deliverable 2.1: Modelling Electric Storage Devices for Electric Vehicles* [Online]. Available: http://www.ev-merge.eu/images stories/uploads/MERGE_WP2_D2.1.pdf
[22] K. Qian, C. Zhou, M. Allan, and Y. Yuan, "Modeling of load demand due to EV battery charging in distribution systems," *IEEE Trans. Power Syst.*, vol. 26, no. 2, pp. 802–810, May 2009.
[23] J. Dobals and F. G. Benitez, "An approach to estimating and updating origin-destination matrices based upon traffic counts preserving the prior structure of a survey matrix," *Transp. Res. B Method.*, vol. 39, no. 7, pp. 569–591, Aug. 2005.
[24] S. R. Hu and C. M. Wang, "Vehicle detector deployment strategies for the estimation of network Origin destination demands using partial link traffic counts," *IEEE Trans. Intell. Transp. Syst.*, vol. 9, no. 2, pp. 288–300, Jun. 2008.
[25] B. Seungkirl, K. Hyunmyung, and L. Yongtaek, "Multiple-vehicle origin-destination matrix estimation from traffic counts using genetic algorithm," *J. Transp. Eng.*, vol. 130, no. 3, pp. 339–347, May 2004.
[26] Y. Kudoh *et al.*, "Environmental evaluation of introducing electic vehicles using a dynamic traffic-flow model," *Appl. Energy*, vol. 69, pp. 145–159, 2001.
[27] T. M. Chan, "More algorithms for all-pairs shortest paths in weighted graphs," *SIAM J. Comput.*, vol. 39, no. 5, pp. 2075–2089, Feb. 2010.
[28] Hainan Provincal Bureau of Statistics, National Bureau of statistics Hainan Survey Corps. (2014). *Hainan Statistical Yearbook*, China Statistics Press [Online]. Available: http://www.stats.hainan.gov.cn/2014nj/indexch.htm
[29] J. Rice, "*Mathematical Statistics and Data Analysis*, 2nd ed. USA: Brooks Cole, Duxbury Press, 1995, ISBN 0-534-20934-3.
[30] L. Ertoz, M. Steinbach, and V. Kumar, "A new shared nearest neighbor clustering algorithm and its applications," in *Proc. Workshop Cluster. High Dimension. Data Appl. 2nd SIAM Int. Conf. Data Min.*, Apr. 2002, pp. 1–15.
[31] L. Ertöz, M. Steinbach, and V. Kumar, "Finding clusters of different sizes, shapes, and densities in noisy, high dimensional data," in *Proc. SIAM Int. Conf. Data Min. (SDM)*, May 2003, pp. 47–58.
[32] R. B. Cooper, *Introduction to Queuing Theory*. Amsterdam, The Netherlands: North Holland, 1981.
[33] A. O. Allen, *Probability, Statistics, and Queuing Theory*. New York, NY, USA: Academic Press, 2014.
[34] F. B. Nilsen. (1998). *Queuing Systems: Modeling, Analysis and Simulation*, Research report [Online]. Available: http://urn.nb.no/URN:NBN:no-18972
[35] D. Liu, T. Qi, K. Zhang, and Y. Guo, "Beijing residents' travel time survey in small samples," *J. Transp. Syst. Eng. Inf. Technol.*, vol. 9, no. 2, Apr. 2009, pp. 23–26.
[36] The State Council. (2009, Dec.). *Several Opinions on Promoting the Constructing of Hainan International Tourism Island* [Online]. Available: http://www.gov.cn/zwgk/2010-01/04/content_1502531.htm

Xiaohong Dong was born in Hebei, China. She is currently pursuing the Ph.D. degree at Tianjin University, Tianjin, China. Her research interests include electric vehicle charging infrastructure planning and power system stability analysis.

Yunfei Mu (M'11) was born in Hebei, China. He received the Ph.D. degree from the School of Electrical Engineering and Automation, Tianjin University, Tianjin, China, in 2012. He is now an Associate Professor with Tianjin University. His research interests include power system security analysis, electric vehicles, and smart grids.

Hongjie Jia (M'04) was born in Hebei, China. He received the B.S., M.S., and Ph.D. degrees in electrical engineering from Tianjin University, Tianjin, China, in 1996, 1998, and 2001, respectively. He is a Professor with Tianjin University. His research interests include power system stability analysis and control, distribution network planning, renewable energy integration, and smart grids.

Jianzhong Wu (M'06) received the Ph.D. degree from Tianjin University, Tianjin, China, in 2004. Then, he was worked with Tianjin University from 2004 to 2006. He was a Research Fellow with the University of Manchester, Manchester, U.K., from 2006 to 2008. He is currently a Professor with Institute of Energy, Cardiff School of Engineering, Cardiff, U.K. His research interests include focused on energy infrastructure and smart grids.

Xiaodan Yu was born in Liaoning, China. She received the B.S., M.S., and Ph.D. degrees in the electrical engineering from Tianjin University, Tianjin, China, in 1996, 1998, and 2013, respectively. She is an Associate Professor with Tianjin University. Her research interests include power system stability analysis, nonlinear dynamic circuit, and the optimal operation of power system.